

The WIMP annual modulation signal and non-standard halo models

Anne M. Green

Astronomy Unit, School of Mathematical Sciences, Queen Mary and Westfield College, Mile End Road, London, E1 4NS, UK
(December 2, 2024)

Currently the best prospect for detecting Weakly Interacting Massive Particles (WIMPs) is via the annual modulation, which occurs due to the Earth's rotation around the Sun, of the direct detection signal. We investigate the effect of uncertainties in our knowledge of the structure of the galactic halo on the WIMP annual modulation signal. We evaluate the signal for three non-standard halo models: Evans' power-law halos, Michie models with an asymmetric velocity distribution and Maxwellian halos with bulk rotation. We then compare the theoretical predictions of these models with the experimental signal found by the DAMA experiment and investigate how the WIMP mass and interaction cross section determined depend on the halo model assumed. We find that the WIMP mass confidence limits are significantly extended to larger masses, with the shape of the allowed region in the mass-cross section plane depending on the model.

98.70.V, 98.80.C

I. INTRODUCTION

The rotation curves of spiral galaxies are typically flat out to about ~ 30 kpc. This implies that the mass enclosed increases linearly with radius, with a halo of dark matter extending beyond the luminous matter [1]. The nature of the dark matter is unknown [2], with possible candidates including Massive Compact Halo Objects (MACHOs), such as brown dwarves, Jupiters or black holes and elementary particles, known as Weakly Interacting Massive Particles (WIMPs), such as axions and the neutrino, the lightest supersymmetric particle.

WIMPs can be directly detected via their elastic scattering off target nuclei. In the long term the directional dependence of the detector recoil will provide the best means of direct WIMP detection [3]. Currently the best prospect for distinguishing a WIMP signal from the detector background is via the annual modulation of the signal, which occurs due to the Earth's rotation around the sun [4,5]. The DAMA collaboration [6], using a detector consisting of radiopure NaI crystal scintillators at the Gran Sasso Laboratory, have recently reported a 4σ annual modulation signal consistent with the detection of a WIMP with mass $m_\chi = 52^{+10}_{-8}$ GeV [7], assuming a Maxwellian halo with velocity dispersion roughly equal to the local rotation velocity, $v_0 = 220 \text{ km s}^{-1}$.

The values of the WIMP mass and interaction cross section found from the annual modulation signal are known to depend somewhat on the assumed values of poorly known astrophysical parameters. The effects of bulk rotation [8,9] and varying the velocity dispersion [10,9], within the observationally allowed range $v_0 = 220 \pm 40 \text{ km s}^{-1}$ [11], have been examined for a Maxwellian halo. The DAMA collaboration have subsequently included these uncertainties in the analysis of their latest data [7].

The standard Maxwellian halo model has a number of deficiencies (for example see Ref. [12] and references

therein). The halo may not be spherical; N body simulations of gravitational collapse produce axisymmetric or triaxial halos, and indeed other spiral galaxies appear to have flattened halos [13]. The power-law halo models of Evans [14] provide an analytically tractable framework for investigating the effect of varying halo properties such as the flattening, and have previously been used to investigate variations in the mean total [15] and directional [3] WIMP detection rates. Another possible modification to the standard halo model is an asymmetric velocity distribution [4] and the annual modulation of the total [16,17] and directional [16] WIMP signals have been calculated for various asymmetric velocity distributions.

In this paper we investigate the variation of the annual modulation signal for power-law halo models, asymmetric velocity distributions and Maxwellian halos with bulk rotation. We then examine how the range of WIMP masses consistent with the latest DAMA data depends on the halo model assumed.

II. ANNUAL MODULATION SIGNAL

The WIMP detection rate depends on the speed distribution of the WIMPs in the rest frame of the detector, f_v . This is found from the halo velocity distribution, $f(\mathbf{v})$ by making a Galilean transformation $\mathbf{v} \rightarrow \tilde{\mathbf{v}} = \mathbf{v} + \mathbf{v}_e$, where \mathbf{v}_e is the Earth's velocity relative to the galactic rest frame, and then integrating over the angular distribution. In galactic co-ordinates the axis of the ecliptic lies very close to the $\phi - z$ plane and is inclined at an angle $\gamma \approx 29.80^\circ$ to the $\phi - r$ plane [16]. Including all

*The effect of the Sun's gravity on the WIMP distribution can be neglected [18].

components of the Earth's motion, not just that parallel to the galactic rotation:

$$\mathbf{v}_e = v_1 \sin \alpha \hat{r} + (v_0 + v_1 \cos \alpha \sin \gamma) \hat{\phi} - v_1 \cos \alpha \cos \gamma \hat{z}, \quad (1)$$

where $v_0 \approx 232 \text{ km s}^{-1}$ is the speed of the sun with respect to the galactic rest frame, $v_1 \approx 30 \text{ km s}^{-1}$ is the orbital speed of the Earth around the Sun and $\alpha = 2\pi(t - t_0)/T$, with $T = 1$ year and $t_0 \sim 153$ days (June 2nd), when the component of the Earth's velocity parallel to the Sun's motion is largest.

In the range of masses and interaction cross sections accessible to current direct detection experiments the best motivated WIMP candidate is the neutrino, for which the event rate is dominated by the scalar contribution. The differential event rate can then be written in terms of the WIMP cross section on the proton,

$$\sigma_p = \frac{4m_p^2 m_\chi^2}{\pi(m_p + m_\chi)^2} f_p^2, \quad (2)$$

where m_p is the proton mass and f_p the effective WIMP cross section on the proton. The differential event rate simplifies to (see the Appendix for more details):

$$\frac{dR}{dE} = \xi \sigma_p \left[\frac{\rho_{0.3}}{\sqrt{\pi} v_0} \frac{(m_p + m_\chi)^2}{m_p^2 m_\chi^3} A^2 T(E) F^2(q) \right], \quad (3)$$

where the local WIMP density, ρ_χ has been normalised to a fiducial value $\rho_{0.3} = 0.3 \text{ GeV/cm}^3$, such that $\xi = \rho_\chi / \rho_{0.3}$, E is the recoil energy of the detector nucleus and $T(E)$ is defined as [19]

$$T(E) = \frac{\sqrt{\pi} v_0}{2} \int_{v_{\min}}^{\infty} \frac{f_v}{v} dv, \quad (4)$$

where v_{\min} is the minimum detectable WIMP velocity

$$v_{\min} = \left(\frac{E(m_\chi + m_A)^2}{2m_\chi^2 m_A} \right)^{1/2}, \quad (5)$$

and m_A the atomic mass of the target nuclei.

In order to compare the theoretical signal with that observed we need to take into account the response of the detector. The electron equivalent energy, E_{ee} , which is actually measured is a fixed fraction of the recoil energy: $E_{ee} = q_A E$. The quenching factors for I and Na are $q_I = 0.30$ and $q_{Na} = 0.09$ respectively [20]. The energy resolution of the detector [8] is already taken into account in the data released by the DAMA collaboration.

The expected experimental spectrum per energy bin for the DAMA collaboration set-up is then given by [10]

$$\begin{aligned} \frac{\Delta R}{\Delta E}(E) = & r_{Na} \int_{E/q_{Na}}^{(E+\Delta E)/q_{Na}} \frac{dR_{Na}}{dE_{ee}}(E_{ee}) \frac{dE_{ee}}{\Delta E} \\ & + r_I \int_{E/q_I}^{(E+\Delta E)/q_I} \frac{dR_I}{dE_{ee}}(E_{ee}) \frac{dE_{ee}}{\Delta E}, \end{aligned} \quad (6)$$

Energy (keV)	$S_{0,k}$ (cpd/kg/keV)	$S_{m,k}$ (cpd/kg/keV)
2-3	0.54 ± 0.09	0.023 ± 0.006
3-4	0.21 ± 0.05	0.013 ± 0.002
4-5	0.08 ± 0.02	0.007 ± 0.001
5-6	0.03 ± 0.01	0.003 ± 0.001

TABLE I. $S_{0,k}$ and $S_{m,k}$ values obtained, by the DAMA collaboration, from a maximum likelihood analysis of their combined data from four annual cycles.

where $r_{Na} = 0.153$ and $r_I = 0.847$ are the mass fractions of Na and I respectively.

Since $v_0 \gg v_1$ the differential event rate in the k -th energy bin can be expanded in a Taylor series in $\cos \alpha$ [21]:

$$\frac{\Delta R}{\Delta E}(E_k) \approx S_{0,k} + S_{m,k} \cos \alpha. \quad (7)$$

The DAMA collaboration use a maximum likelihood method to separate the time-independent background from the WIMP signal and have released the resulting values of $S_{0,k}$ and $S_{m,k}$, and the errors on them, for each energy bin [7] (see Table 1).

III. HALO MODELS

Since the resolution of numerical simulations is not yet large enough to allow the numerical calculation of the annual modulation signal [22], we have to use analytic models for the velocity distribution of the dark matter halo. If the galactic halo contains large amounts of substructure, as N-body simulations appear to indicate [23], then the WIMP detection rate may be dramatically altered if we are currently passing through a clump of substructure. The extent to which substructure is actually present in the halo is currently a matter of debate however.

The effect of the halo model on the annual modulation signal can be assessed most simply, with least recourse to the detector properties, in terms of the dimensionless function $T(E)$, as defined in Eq. (4). For each model we plot the mean value of $T(E)$, $T(E)_{av}$, and the annual variation,

$$\Delta T(E) = \frac{(T(E)_{\max} - T(E)_{av})}{T(E)_{av}}, \quad (8)$$

defined such that $\Delta T(E)$ is taken to be positive if $T(E)$ is largest in June ($\alpha = 0$) as found by the DAMA collaboration, as a function of recoil energy for a Ge^{76} detector and four values of the WIMP mass: $m_\chi = 30, 50, 100, 200$ GeV. Values for other monatomic detectors can be found by rescaling the x-axis by $m_A/(m_A + m_\chi)^2$. For the NaI detector used by the DAMA collaboration, for $E_{ee} < 6$ keV, equivalent to $E < 20$ keV taking quenching into account, the detector response is dominated by I^{127} [24].

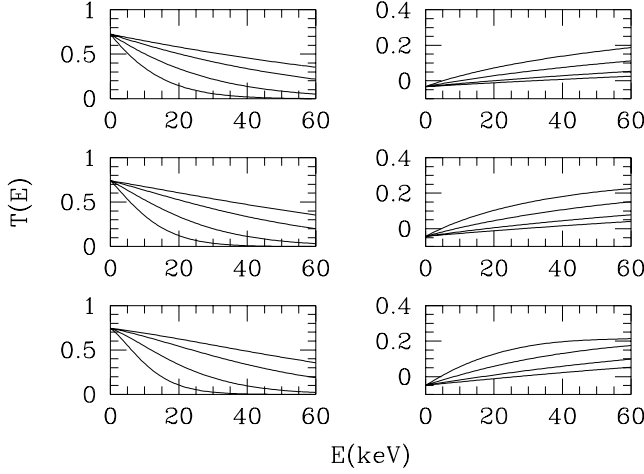


FIG. 1. The mean value (annual variation) of $T(E)$ for halo models with asymmetric velocity distributions with $\lambda = 0, 0.5, 1$, from top to bottom row, for four values of the WIMP mass $m_\chi = 30, 50, 100, 200$ GeV, from top to bottom (bottom to top) within each panel in the left (right) hand column.

The necessary rescaling factor is then roughly 0.76 for $m_\chi = 30$ GeV increasing to 1.2 for $m_\chi = 200$ GeV.

A. Asymmetric velocity distribution

An extension of the Michie model can be used as a simple model of velocity anisotropy [4,16]

$$f(\mathbf{v}) = N \left[\exp\left(-\frac{v^2}{\sigma^2}\right) - \exp\left(-\frac{v_{\text{esc}}^2}{\sigma^2}\right) \right] \times \exp\left(-\lambda \frac{v_\phi^2 + v_z^2}{\sigma^2}\right), \quad (9)$$

where v_{esc} is the escape velocity and N is a normalisation constant. The deviation of the velocity distribution from isotropic is parameterised by λ , the standard Maxwellian halo, cut-off at the escape velocity, is recovered for $\lambda = 0$. Since the halo is formed by gravitational collapse the deviation is most likely to be towards radial orbits, with $0 < \lambda < 1$ [4]. We take $v_{\text{esc}} = 650 \text{ km s}^{-1}$, although the effect of variations in the value of the escape velocity is small [4,9].

The mean value of $T(E)$, $T(E)_{\text{av}}$, and the annual variation, $\Delta T(E)$, are plotted in Fig. 1 for $\lambda = 0, 0.5, 1$. The mean value is higher for the asymmetric models than for the standard Maxwellian halo model. The fractional change in the mean value, relative to that for the Maxwellian halo model, increases with increasing recoil energy and is largest for small WIMP masses. The fractional change in the annual variation is far larger than that in the mean value.

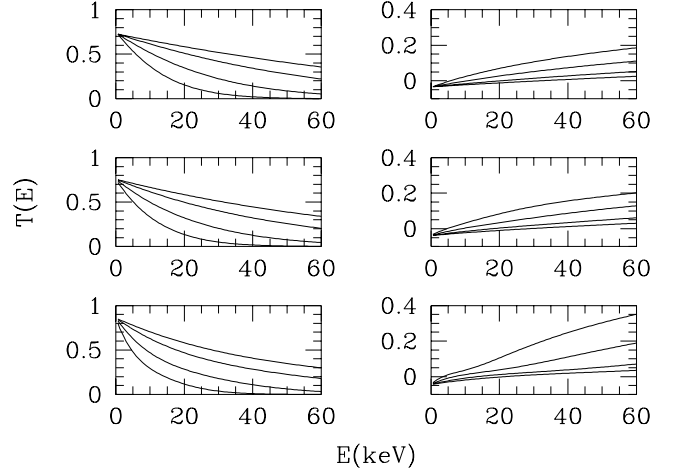


FIG. 2. The mean value (annual variation) of $T(E)$ for power-law halos with $q = 1, 0.85, 0.707$, from top to bottom row, for four values of the WIMP mass $m_\chi = 30, 50, 100, 200$ GeV, from top to bottom (bottom to top) within each panel in the left (right) hand column.

B. Power-law halos

Evans' family of axisymmetric distribution functions [14] lead to velocity distribution functions, in the rest frame of the galaxy, of the form [15]:

$$f(\mathbf{v}) = (AR^2v_\phi^2 + B) \frac{\exp[-2(v/v_0)^2]}{(R^2 + R_c^2)^2} + \frac{\exp[-2(v/v_0)^2]}{R^2 + R_c^2}, \quad (10)$$

with

$$A = \left(\frac{2}{\pi}\right)^{5/2} \frac{(1-q^2)}{Gq^2v_0^3}, B = \left(\frac{2}{\pi^5}\right)^{1/2} \frac{R_c}{Gq^2v_0}, C = \frac{2q^2 - 1}{4\pi Gq^2v_0}, \quad (11)$$

where R_c is the core radius, R_0 is the solar radius and q is a flattening parameter, which varies between 1, for spherical halo, and $1/\sqrt{2} = 0.707$. Following Ref. [15] we take $R_c = 8.5 \text{ kpc}$ and $R_0 = 7 \text{ kpc}$ and explore the effect of varying q . The standard Maxwellian halo is recovered for $q = 1$.

The mean value of $T(E)$, $T(E)_{\text{av}}$, and annual deviation, $\Delta T(E)$, are plotted in Fig. 2 for $q = 1, 0.85, 0.707$. The mean value is lower for the flattened halos than for the Maxwellian halo. The fractional change in the mean value, relative to that for the Maxwellian halo model, increases with increasing recoil energy and is largest for small WIMP masses. The change in the annual variation due to flattening is larger than that due to an asymmetric velocity distribution, particularly so for large recoil energies and small WIMP masses.

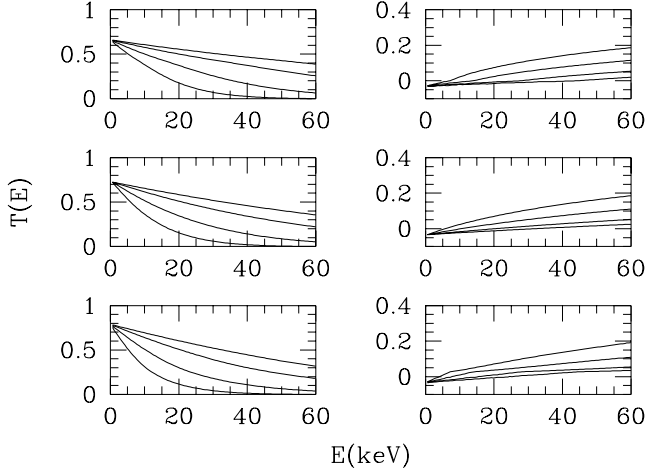


FIG. 3. The mean value (annual variation) of $T(E)$ for rotating Maxwellian halo models with $a_{\text{rot}} = 0.36, 0.5, 0.64$, from top to bottom row, for four values of the WIMP mass $m_\chi = 30, 50, 100, 200$ GeV, from top to bottom (bottom to top) within each panel in the left (right) hand column.

C. Bulk rotation

Halo models with bulk rotation can be constructed by taking linear combinations of the velocity distribution function [15]:

$$f_{\text{rot}}(\mathbf{v}) = a_{\text{rot}} f_+(\mathbf{v}) + (1 - a_{\text{rot}}) f_-(\mathbf{v}), \quad (12)$$

where

$$f_+(\mathbf{v}) = \begin{cases} f(\mathbf{v}) & v_\phi > 0 \\ 0 & v_\phi < 0 \end{cases} \quad (13)$$

$$f_-(\mathbf{v}) = \begin{cases} 0 & v_\phi > 0 \\ f(\mathbf{v}) & v_\phi < 0 \end{cases} \quad (14)$$

and a_{rot} is related to the dimensionless galactic angular momentum, λ_{rot} : $\lambda_{\text{rot}} = 0.36|a_{\text{rot}} - 0.5|$. Numerical studies of galaxy formation find that $|\lambda_{\text{rot}}| < 0.05$ [25], corresponding to $0.36 < a_{\text{rot}} < 0.64$. A non-rotating halo has $a_{\text{rot}} = 0.5$, whilst a counter-rotating (co-rotating) has $a_{\text{rot}} < 0.5$ ($a_{\text{rot}} > 0.5$).

The mean value of $T(E)$, $T(E)_{\text{av}}$, and annual variation, $\Delta T(E)$, are plotted in Fig. 3 for Maxwellian halos with $a_{\text{rot}} = 0.36, 0.5, 0.64$. The mean value for counter(co)-rotation is lower (higher) than for the non-rotating Maxwellian halo at small recoil energies, and higher (lower) at large recoil energies. The change in the annual variation, which is suppressed (enlarged) for counter(co)-rotation, is largest for small recoil energies.

For each of the halo models studied the mean signal decreases most rapidly with increasing recoil energy for small WIMP masses. The annual variation is negative for small recoil energies ($E \lesssim 4$ keV for $M_\chi = 30$ GeV, $E \lesssim$

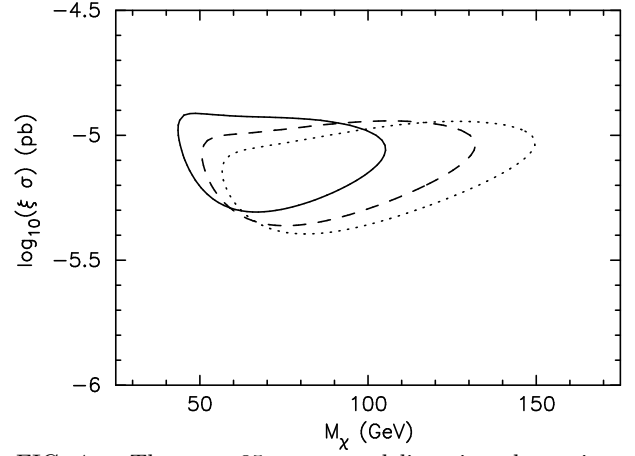


FIG. 4. The $\kappa = 35$ contour, delineating the region of $m_\chi - \xi\sigma$ parameter space compatible with the DAMA annual modulation signal, for asymmetric halo models with $\lambda = 0, 0.5, 1$ (solid, dashed and dotted lines respectively).

30 keV for $M_\chi = 200$ GeV) increasing as the recoil energy increases. For fixed recoil energy the annual deviation is largest for small WIMP masses.

IV. ANALYSIS OF THE DAMA DATA

Brhlik and Roszkowski [10] have devised a technique for comparing the experimental results released by DAMA with theoretical predictions for the annual modulation signal, in the absence of detailed information about the experimental set-up, such as the efficiency of each NaI crystal. They define a function κ :

$$\kappa = \sum_k \frac{(S_{0,k}^{\text{th}} - S_{0,k}^{\text{exp}})^2}{\sigma_{0,k}^2} + \sum_k \frac{(S_{m,k}^{\text{th}} - S_{m,k}^{\text{exp}})^2}{\sigma_{m,k}^2}, \quad (15)$$

where the experimental errors on the time dependent and independent parts of the signal, $\sigma_{m,k}$ and $\sigma_{0,k}$ respectively, serve as weights. The contour, in the $m_\chi - \xi\sigma_p$ plane, $\kappa = 35$ agrees reasonably well with the DAMA collaborations 3σ contour. Whilst this approach does not give accurate confidence limits on m_χ and $\xi\sigma_p$ it does illustrate the qualitative effect of varying the properties of the halo model on the values of the WIMP parameters obtained from the data.

Given the experimental difficulties of extracting a small annual variation from, possibly time dependent, backgrounds, concerns have been expressed about the interpretation of the earlier (1 and 2 year) DAMA data as evidence for a WIMP signal [26]. Furthermore the Cryogenic Dark Matter Search (CDMS) collaboration have recently released limits on the WIMP-Nucleon cross section which exclude, at 85% confidence, the entire DAMA 3σ allowed region [27]. The DAMA collaboration have, however, performed a thorough analysis of the various sources of possible systematic errors [28] and, since the

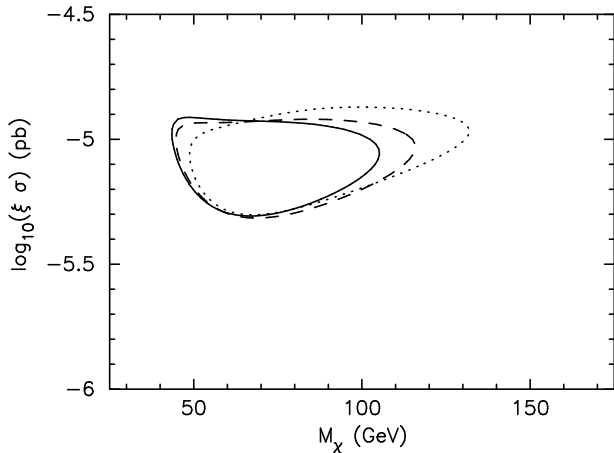


FIG. 5. The $\kappa = 35$ contour for flattened halo models with $q = 1.0, 0.85, 0.707$ (solid, dashed and dotted lines respectively).

DAMA and CDMS experiments use different target nuclei, assumptions are required to perform a direct comparison. In any case even if the interpretation of the DAMA annual modulation signal as WIMP scattering is eventually found to be erroneous, our results will still indicate the qualitative effect of non-standard halo models on the analysis of a WIMP annual modulation signal.

In Figs. 4- 6 we plot contours of $\kappa = 35$, delineating the region of m_χ - $\xi\sigma$ parameter space compatible with the DAMA annual modulation signal, for asymmetric, flattened and rotating halo models respectively. In Fig. 4 we see that as the asymmetry of the velocity distribution is increased the allowed region is enlarged and moves to larger masses and slightly smaller interaction cross sections. We saw in Fig. 2 that the change in the annual modulation signal due to flattening of the halo is larger than that due to velocity asymmetry. Consequentially the change in the allowed region due to flattening is smaller, extending to larger masses and slightly larger interaction cross sections. In Fig. 6 we can see that counter-rotation ($a_{\text{rot}} < 0.5$) contracts the allowed region and shifts it to smaller cross sections whilst co-rotation ($a_{\text{rot}} > 0.5$) expands it and shifts it to larger cross sections. This is in good agreement with the results of Ref. [9] on the effect of bulk rotation, which were found via a full likelihood analysis of the DAMA data.

V. CONCLUSIONS

In this paper we have examined the effect of an asymmetric halo velocity distribution, halo flattening and bulk halo rotation on the WIMP annual modulation signal. Whilst for each of the halo models the change in the mean signal is small, $< 10\%$ for the range of recoil energies probed by the DAMA experiment, the amplitude of the annual modulation can change significantly. The magnitude of the change depends on the WIMP mass

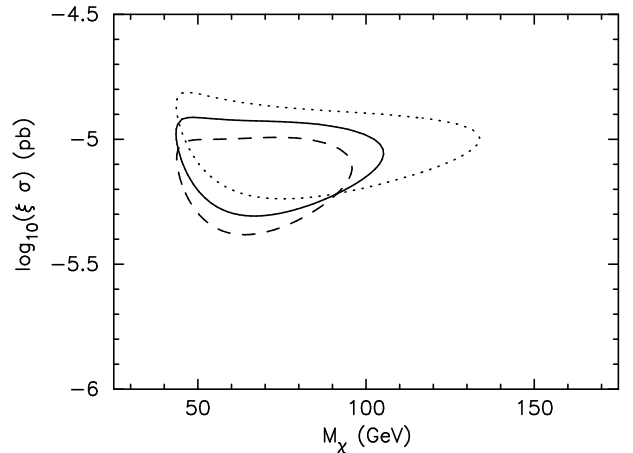


FIG. 6. The $\kappa = 35$ contour for the standard halo model with $a_{\text{rot}} = 0.36, 0.5, 0.64$ (dashed, solid and dotted lines respectively). The non-rotating halo corresponds to $a_{\text{rot}} = 0.5$.

and recoil energy, as well the nature of the deviation of the halo model from the standard Maxwellian halo. With bulk rotation the change in the annual variation, relative to the Maxwellian halo model, is largest for small recoil energies, whilst halo flattening produces the largest change for larger recoil energies.

The range of WIMP masses consistent with the DAMA annual modulation signal is enlarged significantly, to roughly $30 < m_\chi < 150$ GeV at 3σ , for each of the models considered. The shape of the allowed region in the $m_\chi - \xi\sigma_p$ plane is different for each model however. This indicates that the uncertainties in halo modelling have a significant effect on the WIMP mass determined from the annual modulation signal. Therefore more sophisticated halo models (such as those in Ref. [29]) need to be developed and used in the analysis of annual modulation data.

ACKNOWLEDGMENTS

The author is supported by PPARC and acknowledges the use of the Starlink facilities at QMW. The author would also like to thank J. D. Vergados for useful discussions.

APPENDIX A: INTERACTION CROSS SECTION

The differential cross section for neutrino scattering off a target nucleus is dominated by the scalar and axial terms [30,19,10]:

$$\frac{d\sigma}{d\mathbf{q}^2} = \frac{d\sigma^{\text{scalar}}}{d\mathbf{q}^2} + \frac{d\sigma^{\text{axial}}}{d\mathbf{q}^2}, \quad (\text{A1})$$

where $\mathbf{q} = (m_A m_\chi)/(m_A + m_\chi)\mathbf{v}$ is the momentum transferred.

The scalar differential cross section, which arises due to Higgs boson and squark exchange, is given by [19]

$$\frac{d\sigma^{\text{scalar}}}{d\mathbf{q}^2} = \frac{1}{\pi v^2} [Zf_p + (A - Z)f_n]^2 F^2(q), \quad (\text{A2})$$

where f_p and f_n are the effective neutrino couplings to the proton and the neutron respectively and $F(q)$ is the scalar nuclear form factor. The form factor for Na is usually taken to be equal to unity, whilst for I the Saxon-Woods form factor [31]

$$F(q) = \frac{3j_1(qR_1)}{qR_1} \exp[-(qs)^2/2], \quad (\text{A3})$$

where $R_1 = \sqrt{R_A^2 - 5s^2}$, $R_A = A^{1/3} \times 1.2\text{fm}$ and $s = 1\text{fm}$, is used.

The axial differential cross section, which arises due to Z_0 and squark exchange, is given by [19]

$$\frac{d\sigma^{\text{axial}}}{d\mathbf{q}^2} = \frac{8}{\pi v^2} \Lambda^2 J(J+1) S(q), \quad (\text{A4})$$

where J is the total angular momentum, $S(q)$ is the spin form factor and Λ depends on the axial couplings of the neutrino to the quarks (see Ref. [19] for more details and explicit expressions).

The differential event rate for a given detector can then be expressed as [19]:

$$\frac{dR}{dE} = \frac{4}{\pi^{3/2}} \frac{\rho_\chi}{m_\chi} T(E) \times \{[Zf_p + (A - Z)f_n]^2 F^2(q) + 8\Lambda^2 J(J+1) S(q)\}. \quad (\text{A5})$$

[1] K. M. Ashman, Publ. Astron. Soc. Pac., 104, 1109 (1992); C. J. Kochanek, Astrophys. J. **445**, 559 (1995).
[2] J. R. Primack, B. Sadoulet and D. Seckel, Ann. Rev. Nucl. Part. Sci., B38, 751 (1988).
[3] C. J. Copi, J. Heo and L. M. Krauss, Phys. Lett. **B461**, 43 (1999).
[4] A. K. Drukier, K. Freese and D. N. Spergel, Phys. Rev. D **33**, 3495 (1986).
[5] K. Freese, Phys. Rev. D **37**, 3388 (1988).
[6] R. Bernabei et. al. Phys. Lett. **B389**, 757 (1996); *ibid* **B408**, 439 (1997); *ibid* **B424**, 195 (1998); *ibid* **B450**, 448 (1999).
[7] R. Bernabei et. al. Phys. Lett. **B480**, 23 (2000).
[8] F. Donato, N. Fornengo and S. Scopel, Astropart. Phys. **9**, 247 (1998).
[9] P. Belli et. al. Phys. Rev. D **61**, 023512 (2000).
[10] M. Brhlik and L. Roszkowski, Phys. Lett. **B464**, 303 (1999).

[11] P. J. T. Leonard and S. Tremaine, Astrophys. J. **353**, 486 (1990); K. M. Cudworth, Astron. J. **99**, 590 (1990); C. S. Kochanek, Astrophys. J. **457**, 228 (1996).
[12] C. Alcock et. al. Astrophys. J., **449**, 28 (1995).
[13] P. D. Sackett et. al. Astrophys. J., **436**, 629 (1994).
[14] N. W. Evans, Mon. Not. Roy. Astron. Soc., **260**, 191 (1993); *ibid*. **267**, 333 (1994).
[15] M. Kamionkowski and A. Kinkhabwala, Phys. Rev. D **57**, 3256 (1998).
[16] J. D. Vergados, Phys. Rev. Lett. **83**, 3597 (1999); Phys. Rev. D **62**, 023519 (2000).
[17] P. Ullio and M. Kamionkowski, hep-ph/0006183.
[18] K. Griest, Phys. Rev. D **37**, 2703, (1988).
[19] G. Jungman, M. Kamionkowski and K. Griest, Phys. Rep. **267**, 195 (1996).
[20] K. Fushimi et. al. Phys. Rev. C **47**, R245 (1993); G. J. Davies et. al. Phys. Lett. **B322**, 159 (1994); P. F. Smith et. al. Phys. Lett. **B379**, 299 (1996).
[21] K. Freese, J. Frieman and A. Gould, Phys. Rev. D **37**, 3388 (1988).
[22] L. M. Widrow and J. Dubinski Astrop. J., **504**, 12 (1998).
[23] J. F. Navarro, C. S. Frenk and S. D. M. White, Astrophys. J. **462**, 563 (1996); B. Moore et. al. Mon. Not. R. Astron. Soc. **310** (1999), 1147; A. V. Kravtsov et. al. Astrophys. J. **502**, 48 (1998).
[24] A. Bottino, V. de Alfaro, N. Fornengo, G. Mignola and S. Scopel, Astropart. Phys. **2**, 67 (1994).
[25] J. Barnes and G. Efstathiou, Astrophys. J. **319**, 575 (1987); M. S. Warren, P. J. Quinn, J. K. Salomon and W. H. Zurek, Astrophys. J. **399**, 405 (1992); S. Cole and C. Lacey, Mon. Not. R. Astron. Soc. **281**, 716 (1996).
[26] G. Gerbier, J. Mallet, L. Mosca and C. Tao, astro-ph/9710181; astro-ph/9902194.
[27] CDMS Collaboration, Nucl. Instrum. Meth. **A444** 345 (2000); Phys. Rev. Lett. **84**, 5699 (2000).
[28] R. Bernabei et. al. preprint ROM2F/2000-15, to appear in the proceedings of the International Workshop DM2000, Marina del Rey.
[29] N. W. Evans, C. M. Carollo and P. T. de Zeeuw, astro-ph/0008156.
[30] M. Goodman and E. Witten, Phys. Rev. D **31**, 3059 (1985).
[31] J. Engel, Phys. Lett. **B264**, 114 (1991).